Targeted glycophagy ATG8 therapy for diabetic heart disease

K M. Mellor,[1,2,3] U. Varma,[3] P. Koutsifeli,[1] C.L. Curl,[3] J.V. Janssens,[3,4] L.J. Daniels,[1] G.B. Bernasochi,[3] A..J.A. Raaijmakers,[3] M. Annandale,[1] X. Li,[1] S.L. James,[1] D.J. Taylor,[4] K. Raedschelders,[4] K.L. Weeks,[3,5] R.J. Mills,[6] R.G. Parton,[7] X. Hu,[10] J.R. Bell,[3,8] E.R. Porrello,[3,6] J.E. Hudson,[9] R-P. Xiao,[10] J.E. Van Eyk,[4] R.A. Gottlieb,[4] L.M.D. Delbridge[3,1]*

Affiliations:
[1]Department of Physiology, University of Auckland, Auckland, New Zealand.
[2]Auckland Bioengineering Institute, University of Auckland, Auckland, New Zealand.
[3]Department of Anatomy and Physiology, University of Melbourne, Melbourne, Victoria, Australia.
[4]Cedars-Sinai Medical Center, Los Angeles, California, USA.
[5]Baker Department of Cardiometabolic Health, University of Melbourne, Melbourne, Victoria, Australia.
[6]Murdoch Children's Research Institute, Melbourne, Victoria, Australia.
[7]Centre for Microscopy and Microanalysis and Institute for Molecular Bioscience, University of Queensland, Brisbane, Queensland, Australia.
[8]Department of Microbiology, Anatomy, Physiology & Pharmacology, La Trobe University, Australia
[9]School of Biomedical Sciences, University of Queensland & QIMR Berghofer, Brisbane, Queensland, Australia
[10]Institute of Molecular Medicine, Peking University, Beijing, China

Keywords: diabetic cardiomyopathy, cardiac metabolism, cardiac glycogen, autophagy, Stbd1, glycogen proteomics, cardiomyocyte stiffness, cardiac organoids

*Corresponding author:
Prof Lea MD Delbridge
lmd@unimelb.edu.au

Diabetic heart disease is highly prevalent[1] and is associated with the early development of impaired diastolic relaxation.[1] The mechanisms of diabetic heart disease are poorly understood and it is a condition for which there are no targeted therapies. Recently, disrupted glycogen-autophagy (glycophagy) and glycogen accumulation have been identified in the diabetic heart.[2] Glycophagy involves glycogen receptor binding and linking with an ATG8 protein to locate and degrade glycogen within an intracellular phago-lysosome.[3,4] Here we show that glycogen receptor protein STBD1 (starch-binding-domain-protein-1) is mobilized early in the cardiac glycogen response to metabolic challenge *in vivo*, and that deficiency of a specific ATG8 linking protein, Gabarapl1 (γ-aminobutyric-acid-receptor-associated-protein-like-1) is associated with diastolic dysfunction in diabetes. Gabarapl1 gene delivery treatment remediated cardiomyocyte and cardiac diastolic dysfunction in type 2 diabetic mice and diastolic performance of 'diabetic' human iPSC-derived cardiac organoids. We identify glycophagy dysregulation as a mechanism and potential treatment target for diabetic heart disease.

Main

Diabetic heart disease is recognized as a distinct cardiomyopathy, characterized by occurrence of diastolic dysfunction.[1] Whilst derangements of cardiomyocyte signaling and functional performance have been described in various forms of diabetic cardiopathology (including types 1 and 2 diabetes),[5,6] the underlying mechanisms which drive the development of diastolic dysfunction and progression to heart failure in diabetes are unclear.

Autophagy is a highly conserved essential catabolic process which involves the breakdown and 'recycling' of defective or surplus cellular materials. An autophagy role in metabolic disease-related heart pathology was first reported more than a decade ago[7,8] describing altered levels of an autophagy intermediate protein in an experimental model of type 2 diabetes. In overview, autophagic processes include receptor tagging of 'cargo' destined for intracellular breakdown. Receptors link with membrane-bound ATG8 family proteins and recruit the molecular machinery to enclose the cargo into an autophagosome. Lysosome fusion with the phagosome allows breakdown and phago-lysosome export of cargo content.[3]

It is now clear that various autophagy receptors and associated ATG8 partners can target specific cellular components. Work in non-muscle cell culture lines has linked a specific glycogen receptor STBD1 (Starch binding domain protein 1) with an ATG8 partner GABARAPL1 (γ GABA type A receptor associated protein like 1).[4,9] Evidence demonstrates that glycogen-selective autophagy ('glycophagy') is operational in the myocardium. Our studies in primary cardiomyocyte cultures have shown STBD1 localization to be distinct and separate to the more extensively characterized ATG8 protein LC3B,[10] which mediates autophagy of protein aggregates via the p62 receptor partner. It has also been shown *in vitro* that cardiomyocyte cellular glycogen levels respond to culture media simulating diabetic hyperglycemic conditions.[10]

As a dense hexose sugar polymer, glycogen constitutes a concentrated glycolysis fuel store. Cardiac glycogen is considered an important energy reserve in physiological settings.[11] Glycolysis is a key energy source in cardiac electro-mechanical transduction, particularly involved in supporting SERCA2-mediated Ca^{2+} reuptake during diastolic relaxation.[12,13] We have recently shown that marked increases in glycogen levels are a consistent feature in a range of diabetic pre-clinical models and in clinically-derived cardiac

tissues.[2] This as yet unexplained phenomenon is cardiac specific – skeletal muscle glycogen levels are not perturbed in basal diabetic pathologic states.[2] Furthermore, cardiac glycogen elevation in rodent diabetic myocardium is associated with electron microscopic visualization of ectopically clustered glycogen particulates amassed adjacent to mitochondria and dispersed throughout the myofilament architecture. In these settings, we have demonstrated that formed and forming glycogen-enriched phagosomes are prominent structures, suggesting cardiomyocyte glycophagy disruption in diabetes.[2] Our recent *in vivo* and *in vitro* studies have shown that myocardial glycophagy flux (i.e. autophagic glycogen throughput) is impaired in diabetes.[2,14]

Thus, in parallel with the well characterized cytosolic enzymatic regulation of glycogen synthesis and breakdown (by glycogen synthase and phosphorylase), glycophagy constitutes a route for 'bulk' homeostatic glycogen handling,[4] susceptible to disruption in diabetes. We hypothesize that in diabetes, disturbance of glycogen processing through glycophagy contributes to cardiac dysfunction, in particular impairing relaxation and diastolic performance. To directly test this proposition, in the present study we sought to determine whether *in vivo* gene manipulation of the key glycophagy ATG8 intermediate (GABARAPL1), has therapeutic potential in diabetic heart disease.

Glycophagy mediator proteins are mobilized early in the cardiac glycogen response to metabolic challenge *in vivo*

Firstly, we used proteomic methods (LC-MS/MS) to explore the cardiomyocyte glycogen receptor - ATG8 homolog relationship, to confirm previous *in vitro* immuno-characterization, and ensure the most efficacious gene targeting approach for glycophagy intervention. STBD1 is known to bind to glycogen at a carbohydrate binding module site (CBM20), and also contains several ATG8-interacting motifs (AIMs). Our *in silico* analyses revealed that 12 glycogen-related proteins contain AIMs (including STBD1) and therefore have the potential to be glycogen receptors to partner with ATG8 proteins.[4] There are 6 ATG8 homologues: the microtubule-associated protein 1A/1B-light chain 3 series (LC3A, LC3B, LC3C); and the γ-aminobutyric acid receptor-associated protein / like1 series (GABARAP, GABARAPL1 and GABARAPL2). Thus potentially numerous receptor-ATG8 combinations are possible.

To contrast the cardiac- and skeletal muscle-specific glycogen proteomes, and to determine whether (and which) CBM20 domain proteins might be present at the earliest

stage of systemic metabolic disturbance, an experimental acute metabolic stimulus was used. A metabolic challenge (MC) was induced in rats with a single dose of streptozotocin (STZ) to lesion pancreatic β cells to suppress insulin secretion. After 48 hours, blood glucose was elevated to more than 20 mM in all treated animals (Ctrl: 6.5 ± 0.2 mM vs. MC: 24.6 ± 0.8 mM). We confirmed significant glycogen elevation in cardiac, but not skeletal muscle tissues (Fig. 1a). Thus cardiac glycogen accumulation was identified as a primary feature of cardiometabolic challenge, and a response evident early after systemic metabolic disturbance. Proteomic analyses were performed on glycogen extracts using liquid chromatography and mass spectrometry (LC-MS/MS). Overall, the cardiac glycogen proteome was more extensive than the skeletal glycogen proteome, comprising a larger number of total identified proteins (513 vs 366 proteins), indicative of increased complexity of the cardiac glycogen regulatory environment (Fig. 1b). For each tissue, amongst the common proteins detected in both control and challenge conditions, a relatively small number showed differential abundance (cardiac n=19, skeletal n=7). Notably, the response to metabolic challenge involved recruitment of unique components to the glycogen proteome in both tissues.

To explore the metabolic characteristics of these tissue-specific responses to metabolic challenge we searched the group of recruited proteins using Gene Ontology terms for Carbohydrate, Fatty Acid and Amino Acid Metabolic Processes (GO:0005975, GO:0006629, GO:0006520). The proteomic profiles generated for each tissue type were markedly different (Fig. 1c), with cardiac muscle proteins showing carbohydrate protein dominance, while fatty acid metabolism-related proteins were more prominent in skeletal muscle. Given that 'lipotoxicity' is a frequent descriptor used in relation to metabolic disturbance in cardiac muscle pathology,[15] this finding was unexpected. These observations indicate that myocardial carbohydrate metabolic derangement has an 'early responder' role in cardiomyocyte glycemic dysregulation.

As an identified glycogen receptor, detection of STBD1 was expected.[4,9,16] Remarkably it was the most abundant protein of the GO 'Carbohydrate Metabolism' term (annotated Fig. 1c), and was recruited to the cardiac proteome in response to metabolic challenge and not the skeletal proteome. Regarding the other 11 known glycogen-related proteins with AIM sequences, glycogen synthase 1 (GYS1), glycogen phosphorylase (PYGM, PYGL, PYGB), and laforin (EPM2A) were detected in cardiac extract but not differentially abundant between metabolic challenge and control. Glycogen synthase 2 (GYS2),

glycogen branching enzyme (AGL), glycogenin 2 (GYG2), glycogen debranching enzyme (GDE), and malin (NHLRC1) were not detected in either extract. Glycogenin 1 (GLYG1) had 25% lower abundance in cardiac glycogen extracted from the metabolic challenge vs control rats. For the pooled group of glycogen-associated proteins uniquely recruited or differentially abundant in the 'carbohydrate metabolic processes' GO category, a map was constructed to compare cardiac and skeletal muscle proteomes (Fig. 1d, Extended Data Table 1). Amongst the 22 proteins detected, STBD1 abundance characteristics were distinctive – under control conditions STBD1 was robustly present in the skeletal glycogen proteome, but not detectable in the cardiac glycogen extracts. In response to the metabolic challenge, while STBD1 was recruited to the cardiac glycogen proteome, the abundance was simultaneously diminished in the skeletal glycogen proteome. The more vigorous cardiac glycogen response to metabolic challenge (vs skeletal muscle) is consistent with clinical findings that cardiac phenotype is most markedly disrupted in a range of somatic genetic conditions described as 'glycogen storage diseases'.[17]

Next, a GO analysis was undertaken (Fig. 1e) to obtain information about higher order functional impacts of metabolic challenge for each tissue using the full sets of differentially abundant and uniquely detected proteins in both treatments (i.e. cardiac n = 64 + 19 + 108 = 191 proteins; skeletal n = 23 + 7 + 159 = 189 proteins (i.e. uniquely control + differentially abundant + uniquely MC)). The cardiac response was characterized by changes in autophagy and glucan catabolic processes in concert with mitochondrial involvement. In contrast, the highest ranked processes in the skeletal muscle response were fatty acid catabolism and oxidative stress. Thus, very different glycogen proteomic metabolic responses were observed in different tissues of the same animals exposed to *in vivo* systemic metabolic challenge induced by acute insulin depletion. Collectively, these proteomic data obtained by targeting the earliest phase of systemic metabolic disturbance reveal that cardiac and skeletal glycogen management processes are fundamentally disparate. The metabolic response pattern in this acute setting, associated with elevation of myocardial glycogen, is consistent with the observed chronic state of glycogen accumulation in diabetic heart disease and suggests potential for disease causation. Augmented STBD1 recruitment to the cardiac glycogen proteome emerges as a crucial point of difference in determining the unique cardiac-patho-phenotype in the initial response to deranged systemic metabolism.

Based on the glycogen proteome data, we next performed a functional network analysis to probe the possible links between glycogen receptor and autophagosome ATG8 effector proteins in metabolic challenge. The STRING database (Search Tool for Retrieval of Interacting Genes/Proteins) captures experimental evidence and performs text-mining to identify evidence of direct and indirect protein-protein associations. Using STBD1 as the input protein, an association network was generated and depicted (Fig. 1f) to illustrate primary (direct, black outline) and secondary protein interactions and designated links of specific evidence type.

GABARAPL1, emerged as the only autophagy protein with direct link to STBD1. This *in silico* finding is supported by recent experimental work resolving the crystal structure of the STBD1 CMB20 interactions with ATG8 family proteins. Structural data demonstrated a binding preference of STBD1 with GABARAPL1. It was also determined that the two oligosaccharide binding sites of STBD1 can (uniquely) accommodate glucose polymer structures involving both the α-1,4- and α-1,6-glycosidic bond types, corresponding to linear and branched glycogen configurations.[18]

Cumulatively these functional proteomic investigations confirm this receptor-Atg8 relationship to constitute a prominent cardiac glycogen autophagy axis. Based on these findings, and a growing general understanding of phagosome mechanisms,[3,4,19] cardiac glycophagy can be conceptualized to comprise several stages: the initial STBD1 receptor attachment to glycogen (CBM20 domain); the glycogen-attached receptor linking to GABARAPL1 at the forming autophagosome membrane (via an ATG8-Interacting Motif, AIM); membrane enclosure of glycogen cargo, and subsequent fusion of the auto-phagosome with a lysosome (containing acid α-glucosidase, GAA) to degrade glycogen generating hexose sugar for cell recycling (Fig. 1g).

Cardiac GabarapL1 (Atg8) deficiency is associated with diastolic dysfunction in diabetes

Next, we investigated the link between glycogen, glycophagy and diastolic dysfunction in established diabetes. Given the known cardiac contractile deficits associated with diabetes,[20] we tested whether a functional association with cardiac glycogen elevation could be identified in a chronic type 2 diabetic (T2D) setting. A high fat (with high sugar) dietary treatment was used to provide a clinically-relevant T2D model of glucose

intolerance, mild hyperglycemia, and obesity (Extended Data Table 2), opting for a more moderate hyperglycemia than can be evident in other rodent models of T2D (e.g. ZDF, db/db).[21] This investigation acquired matching echo data derived *in vivo* with glycogen analysis of tissues recovered post-mortem. Cardiac glycogen content was elevated in T2D mice (Fig. 2a) in the absence of changes in glycogen synthase and glycogen phosphorylase (Extended Data Fig. 1c-e). Diastolic dysfunction *in vivo*, as typically indexed by elevated ratio of the mitral blood flow/tissue displacement Doppler signals (E/e'), was apparent in T2D mice (Fig. 2a, Extended Data Fig. 1b). The elevated E/e' levels recorded were proportionally commensurate with shifts reported in patients with type 2 diabetes.[22] A significant correlation between glycogen and diastolic dysfunction was demonstrated (Fig. 2a). No evidence of altered systolic function (including ejection fraction, fractional shortening) was detected (Extended Data Fig. 1a-b). Given our previous report that cardiac glycophagy flux is impaired in diabetes,[2] we evaluated the expression level of the key glycophagy-mediator genes, *Stbd1*, *Gabarapl1* and *Gaa* to identify the optimal target for gene therapy intervention.

Gene expression levels of *Stbd1* and *Gaa* were preserved in T2D mice. In contrast, a dramatic 60% reduction in *Gabarapl1* mRNA was observed (Fig. 2b), suggesting that ATG8 deficiency may be a glycophagy flux limiting factor. Other data indicate that in general, while autophagy receptor proteins are degraded in the phagolysosome, ATG8 proteins are at least partially recycled to the cytosol to supply ongoing phagosome formation.[23,24] Thus, we reasoned that cardiac-directed gene therapy to provide augmented cytosolic GABARAPL1 production could remediate cardiomyocyte glycogen flux dysregulation in diabetes and exert a beneficial effect on diastolic dysfunction.

Initially we tested if *Gabarapl1* overexpression could modulate glycogen accumulation in cardiomyocytes, using a primary cell *in vitro* approach. Cultured neonatal rat ventricular myocytes (NRVMs) were transduced with AAV9-cTnT-Gabarapl1 to generate an *in vitro* setting of *Gabarapl1* overexpression (~1.8 fold increase, Fig. 2e,f). Glycogen accumulation in NRVMs induced by exposure to media containing high glucose[10] was suppressed by AAV-Gab gene delivery, confirming Gabarapl1 as a viable target for 'rescuing' glycogen dysregulation in a simulated diabetic setting. Together, these findings correlating glycogen with diastolic dysfunction *in vivo*, and showing that *Gabarapl1* gene delivery *in vitro* reduced cardiomyocyte glycogen accumulation, supported the contention that an

intervention to promote glycophagy-mediated glycogen degradation in diabetes may have cardiac functional benefit.

AAV Atg8 gene delivery rescues cardiomyocyte and cardiac diastolic dysfunction in diabetic mice

To determine whether cardiac-specific *Gabarapl1* gene delivery could mitigate progression of glycogen accumulation and diastolic dysfunction in diabetes, an AAV9-cTnT-Gabarapl1 (AAV-Gab) viral gene therapy approach was employed using *in vivo* treatment of mice with established diabetic phenotype. AAV-Gab virus titres were injected by tail vein into T2D and control mice after 14 weeks of high fat high sugar dietary treatment (Extended Data Fig. 2a). Mice were monitored for an additional treatment period of 12 weeks. As expected, the cardiac-specific AAV-Gab virus had no effect on systemic measures of body weight, glucose tolerance and hyperglycemia (Fig. 3a,b, Extended Data Table 4). In contrast, *Gabarapl1* gene delivery had a major cardiac effect. T2D-associated cardiac glycogen accumulation was reversed and diastolic dysfunction (i.e. E/e') was normalized in T2D mice injected with AAV-Gab at 12 weeks post-treatment (Fig. 3c-d and Extended Data Fig. 2b). Systolic function was unaffected by diabetes and AAV9 treatment (Extended Data Fig. 2b and Extended Data Table 4). Thus cardiac-targeted *Gabarapl1* gene delivery dramatically suppressed myocardial glycogen accumulation and restored diastolic dysfunction in a dietary model of type 2 diabetes progression.

To identify possible mechanisms of diastolic functional impairment and remediation we evaluated the performance of single cardiomyocytes obtained from the hearts of AAV-Gab & AAV-null mice after the completion of the treatment period (animal age ≥36 weeks). Recently we have demonstrated *in vitro* that a component of diastolic relaxation pathology in cardiometabolic disease can be attributed to impaired mechanical performance of cardiomyocytes.[25] Single intact cardiomyocytes were isolated from *ex vivo* mouse hearts, by enzymatic perfusion & dissociation procedures. Each cardiomyocyte was attached to a pair of glass fibres coated with a bio-adhesive – one fibre used to apply stretch steps and the other to a force transducer. Single cardiomyocyte nano-mechanical properties were measured using a protocol of calibrated stretch steps applied during pacing (as previously described (Extended Data Fig. 2c).[25] Records superimposed from 2 representative cardiomyocytes from each of the AAV-treated groups shows that with each stretch step both the diastolic and systolic force increases. The diastolic force-length relation for each

myocyte was calculated from the gradient of the line fitted to the data points collected prior to transition to a new step (normalized to % stretch relative to initial length, L_0, Fig. 3e). The mean data show that the slope of the end-diastolic force-length relation (nN/%L_0: an index of myocyte 'stiffness') was significantly increased in cardiomyocytes from T2D hearts (more than doubled), and with AAV-Gab treatment the mean stiffness gradient was not different to control (Fig. 3f). These data provide a novel link between cardiomyocyte stiffness and glycophagy disturbance in diabetic heart disease.

AAV Atg8 gene delivery improves diastolic performance in 'diabetic' human iPSC-derived cardiac organoids

To explore the translational potential of *Gabarapl1* gene delivery in improving diastolic dysfunction in diabetic patients, the *Gabarapl1* viral gene delivery approach was applied to human cardiac organoids in an *in vitro* setting of simulated diabetes ('hyperglycemia'). Three-dimensional engineered heart muscle tissues were formed from human pluripotent stem cells, grown in wells around two elastic posts positioned to provide mechanical resistance to contraction[26,27] (Fig. 4a). Confocal microscopy shows α-actinin-stained contractile tissue is evident throughout the cardiac organoid structure (Fig. 4a). With transmission electron microscopy increased glycogen deposits (black particulates throughout the cytosol) were apparent in organoid tissues cultured in high glucose conditions along with evidence of glycophagosome membranous formations (Fig. 4b). High glucose-induced glycogen accumulation was confirmed in the precursor human pluripotent stem cells (Extended Data Fig. 2d). In human cardiac organoids transduced with AAV-Gab, high glucose incubation conditions were linked with delayed force relaxation (diastolic dysfunction), which was normalized with AAV-Gab gene delivery (Fig. 4c,d). In these cardiac organoids, systolic function was preserved under all conditions (Fig. 4e). These data confirm that *Gabarapl1* gene delivery elicits functional rescue in human cardiac organoids, thus strengthening the case for translational potential.

Discussion

In summary, these findings provide compelling evidence that cardiomyocyte specific regulation of glycophagy constitutes a major myocardial metabolic axis of pathophysiologic importance. Here, using a dietary model of type 2 diabetes exhibiting diastolic dysfunction, we show that cardiac-targeted gene therapy delivering the ATG8 family GABARAPL1 partner of STBD1 (the receptor which binds the glycogen cargo for glycophagosome

capture) resolves cardiomyocyte glycogen accumulation and alleviates diastolic dysfunction.

Recently glycophagy has emerged as a selective autophagic route operating in parallel with other autophagy types including macro/aggrephagy (protein aggregates), mitophagy (organelle turnover) and others. It is likely that autophagy pathways involve some ATG8 redundancy and that the cargo capture may be selective but not exclusive. While structural analyses have demonstrated that the STBD1-GABARAPL1 receptor-ATG8 partner pair have the highest binding affinity, other GABARAP-subfamily proteins also exhibit STBD1 binding (albeit at lower affinity[18]). Such redundancy would confer useful metabolic flexibility – a feature of particular importance in the heart.

Disturbed glycophagy is unlikely to be a condition unique to diabetic heart disease, and may be a factor in a range of conditions where diastolic dysfunction is prominent, including familial hypertrophic cardiomyopathies and heart failure with preserved ejection fraction (HFpEF[28]). Systematic studies are required to assess glycophagy status in other cardiac disease phenotypes.

A limitation of this study is the absence of female data. Physiologically, we have previously identified that fasting-induced glycogen accumulation and glycophagy regulation is accentuated in female hearts.[29] Sex/gender-specific studies of glycophagy intervention will be informative. Further work is also required to understand the physiology of glycophagy involvement in electromechanical performance in order to appreciate the pathology of impaired glycophagy flux. A role for glycophagy in glycolysis fuel localization could be considered in future studies.

Almost three decades since Ohsumi's seminal autophagy discovery work[30], to our knowledge, an autophagy-specific therapy has yet to be clinically tested.[31] As autophagy disturbance has been implicated in a broad range of disease conditions (affecting both cell survival and death), a major challenge is to devise a precision approach which avoids generalized negative health impacts. Our demonstration of cardiac-selective glycophagy as a viable treatment target in cardiac metabolic pathology offers potential for development of interventional therapeutic strategies in diabetic heart disease.

Methods

Animals

Animal experiments were performed at the University of Auckland, the University of Melbourne, and Cedars-Sinai Medical Center. All animal experiments were approved by the relevant institutional Animal Ethics Committee and complied with the guidelines and regulations of the Code of Practice for the Care and Use of Animals for Scientific Purposes. Age-matched male animals were randomly assigned to experimental groups and were housed ≥ 2 animals per cage in a temperature controlled environment 21-23 ˚C with 12 hour light/dark cycles. At the start of all experiments, all animals were drug/test naïve. Unless otherwise specified, animals were fed regular chow.

Acute metabolic stress rats

Metabolic stress was induced in male Sprague Dawley rats at 8 weeks of age via a single 55mg/kg tail vein injection of streptozotocin (STZ; Sigma) and monitored for 2 days. Non-fasted blood glucose was determined by tail prick blood collection analysed by accu-chek glucometer.

Type 2 diabetic high fat high sugar diet mice

Obesity and type 2 diabetes was induced in male C57Bl/6J mice by a high fat high sugar dietary intervention commencing at 8-9 weeks of age.[32] After a 1 week transitional feeding period, animals were fed a high fat diet with high sugar (43% kcal from fat, 200g/kg sucrose, SF04-001, Specialty Feeds) or control reference diet (16% kcal from fat, 100g/kg sucrose, custom mouse AIN93G control diet, Specialty Feeds) for 14-15 weeks. High fat-fed mice exhibit obesity, mild hyperglycemia and glucose intolerance (Extended Data Table 2).

Type 2 diabetic high fat high sugar diet mice with AAV-Gabarapl1 gene delivery

To evaluate the effect of cardiac-specific *Gabarapl1* gene delivery in diabetic heart disease, high fat high sugar- and control-fed male C57Bl/6J mice were randomized to treatment group after 14 weeks of the dietary intervention and received a single tail vein injection of 10^{12} gc/mouse AAV9-cTnT-*Gabarapl1* or AAV9-cTnT-Null virus (Vector Biolabs). The mice continued the high fat high sugar or control diet for a further 14 weeks (glycogen analysis) or 28 weeks (cardiomyocyte stiffness analysis).

Human pluripotent stem cell-derived cardiac organoids

Human pluripotent stem cells were maintained and differentiated into cardiomyocytes (hPSC-CMs) as previously described[26,27] with ethical approval from The University of Queensland's Medical Research Ethics Committee under the regulations of the National Health and Medical Research Council of Australia (NHMRC). hPSC-CMs were dissociated and seeded onto gelatin coated coverslips at 100,000 cells/cm^2 in α-MEM GlutaMAX (Thermo Fisher Scientific), 10 % Fetal bovine serum (FBS; Thermo Fisher Scientific), 200 µM L-ascorbic acid 2-phosphate sesquimagnesium salt hydrate (Sigma) and 1 % penicillin/streptomycin (Thermo Fisher Scientific). Human cardiac organoids (hCOs) were generated from hPSC-CMs using Heart-Dyno culture inserts and cultured in maturation media as previously described.[26] To obtain images of contractile protein ultrastructure, organoids were immunostained with alpha-actinin and hoescht blue (DNA stain) and imaged with a confocal microscope. At Day 9 hCOs were treated with AAV9-cTnT-*Gabarapl1* or AAV9-cTnT-Null virus ($5x10^9$ gc/hCO; Vector Biolabs) for 72 hours in maturation media. hCOs were subsequently washed and cultured in control (Ctrl: maturation media with 1 mM glucose with 24 mM mannitol) or simulated hyperglycemic (HG: maturation media with 25 mM glucose) conditions for 4 days. hCO contractile properties and kinetics were assessed as previously described.[26] At the completion of

contraction analysis, a subset of cardiac organoids were fixed for electron microscopy as described previously.[26]

Neonatal rat ventricular myocyte culture

Cardiomyocytes from male and female postnatal day 1-2 Sprague Dawley rat hearts were isolated and cultured as previously described.[10] Ventricular myocytes were isolated by enzymatic dissociation with trypsin and collagenase. Isolated cells were centrifuged (10 minutes, 1000 g), and resuspended in minimum essential media (MEM, Life Technologies) supplemented with 10 % newborn calf serum (NCBS), essential and non-essential amino acids, antibiotic-antimycotic reagent, 2 mM L-glutamine, and MEM vitamins (Life Technologies) and 26 mM $NaHCO_3$ and 98 µM bromo-deoxyuridine (Sigma), and pre-plated for 1.5 hours at 37 ˚C to obtain a cardiomyocyte-rich fraction. Cells were plated at a cell density of 1250 cells/mm^2 and incubated at 37 ˚C with 5 % CO_2. For *Gabarapl1* overexpression studies, following isolation NRVMs were cultured in MEM-NBCS as described above, for 24 hours, then switched to antibiotic-free, serum-free Opti-MEM (Thermo Fisher Scientific) with AAV9-cTnT-*Gabarapl1* or AAV9-cTnT-Null virus (10,000 gc/cell; Vector Biolabs) for 24 hours. Following transduction, NRVMs were cultured for 48 hours in standard DMEM (with supplements as described above, and 5 mM glucose) prior to 24 hours experimental conditions of control glucose (Ctrl: 5 mM glucose, 25 mM mannitol) vs high glucose (HG: 30 mM glucose). At the completion of the experimental period, cells were lysed with RIPA buffer (Thermo Fisher Scientific) for molecular analysis.

Glucose tolerance testing

Glucose tolerance testing was performed in T2D-AAV mice following 6 hours fasting.[33] Baseline blood glucose levels were measured using an Accu-Chek glucometer with a

small blood sample obtained from a needle prick to the tail vein. Glucose (1.5 g/kg body weight) was injected i.p. and blood glucose was measured at 5, 15, 30, 60 and 90 minutes after the glucose injection.

Echocardiography

Animals were anaesthetized with isoflurane and transthoracic echocardiography was performed using the GE Vivid 9 Dimension echocardiography platform with a 15 MHz i13L linear array transducer (GE Healthcare), as previously described.[32] Left ventricular (LV) m-mode two-dimensional echocardiography was performed in parasternal short axis view to measure LV wall and chamber dimensions to derive systolic function parameters: % ejection fraction ((end diastolic volume – end systolic volume)/end diastolic volume) ×100), and % fractional shortening ((LV end diastolic diameter – LV end systolic diameter)/(LV end diastolic diameter) ×100). Pulse wave Doppler and tissue Doppler imaging were acquired from the apical 4 chamber view to assess LV diastolic function parameters: velocity of early mitral inflow (E) and early diastolic velocity of mitral annulus (e′) and E/e′ ratio. Three consecutive cardiac cycles were sampled for each measurement taken, and analysis was performed in a blinded manner.

Mouse cardiomyocyte isolation, Ca^{2+} handling and nano-mechanical analysis

Adult mouse cardiomyocytes were isolated as previously described.[34] To assess myocyte stiffness properties, cardiomyocytes were attached to glass rods (Myotak, Ionoptix) and lifted from the coverslip using motorized micromanipulators (MC1000E, Siskiyou Corporation). Cardiomyocytes were paced (2 Hz, 2.0 mM Ca^{2+}, 37 °C) and subjected to progressive longitudinal stretch (Nano-drive, Mad City Labs). Sarcomere length/shortening and force development (force transducer stiffness 20 N/m; Myostretcher, Ionoptix). Diastolic force-length relationships were constructed by plotting diastolic force against %

cardiomyocyte stretch. All indices were analyzed off-line using IonWizard software (IonOptix) and were determined after averaging 10 steady-state transients for each myocyte.

Molecular analyses

Glycogen content

Glycogen content was measured by digesting an aliquot of tissue homogenate or cell lysate with amyloglucosidase (#10102857001, Roche) at 50 ˚C for 60 minutes in 1 % triton-X, 0.1 M Na acetate, pH 6.0. Following centrifugation at 16,000 g, 4 ˚C for 2 minutes, the supernatant was assayed for glucose concentration using glucose oxidase/peroxidase colorimetric glucose assay with 45 µg/ml o-dianisdine dihydrochloride (Sigma-Aldrich), and absorbance measured at 450 nm. Another tissue homogenate aliquot was processed in parallel without amyloglucosidase to determine background glucose content. Glycogen levels are presented as glucose units (nmol), normalized to protein (mg, determined by Lowry assay) and depicted as relative levels for comparative purposes.

Immunoblotting

Sample protein concentrations were determined using a Lowry assay. Prior to immunoblotting, tissue homogenates were prepared in loading buffer (50 mM Tris-HCl (pH 6.8), 2 % sodium dodecyl sulfate, 10 % glycerol, 0.1 % bromophenol blue and 2.5 % 2-mercaptoethanol), and equal amounts of protein were loaded into the SDS-PAGE gel. Antibodies for the following proteins were used: phosphorylated (Ser641) glycogen synthase (ab81230, Abcam), glycogen synthase (3893, Cell Signaling), phosphorylated (Ser14) glycogen phosphorylase (gift from Dr David Stapleton), and glycogen phosphorylase (gift from Dr David Stapleton). Membranes were incubated with anti-rabbit horseradish peroxidase-conjugated secondary antibody (GE Healthcare). The ECL Prime (Amersham, GE Healthcare) chemiluminescent signal was visualized with a ChemiDoc-

XRS Imaging device and band intensity quantified using ImageLab software (Bio-Rad). Equal protein loading was confirmed by Coomassie staining of polyvinylidene difluoride membranes (Coomassie Brilliant Blue R-250, Bio-Rad).

Quantitative RT-PCR

RNA was extracted from frozen cardiac tissues using the TRIzol® reagent in conjunction with the PureLink™ Micro-to-Midi Total RNA Purification kit (Life Technologies) with on-column DNase treatment (PureLink DNase; Life Technologies). RNA was reverse transcribed as per the manufacturer's instructions (#18080-051; Life Technologies). Real-time PCR was performed using Sybr-Green (Life Technologies) with primer pairs detailed in Extended Data Table 3. The comparative ΔΔCt method was used to analyze the genes of interest as described.

For assessment of viral copy number in AAV9-treated mouse heart tissue, DNA was extracted as per the manufacturer's instructions (K0152, Thermo Fisher Scientific). AAV9-treated mouse heart DNA was subjected to digital droplet qPCR as per the manufacturer's instructions (Biorad) using primers targeting the WPRE component of the viral vector: 5'-CTGGTTGCTGTCTCTTTATGAGGAG-3' (forward) and 5'-CACTGTGTTTGCTGACGCAACC-3' (reverse). Viral copies/ µg DNA was quantified using QuantaSoft™ Analysis Pro.

Glycogen proteomics

Cardiac (left ventricle) and skeletal muscle (quadriceps) tissue was collected from control and acute metabolic stress rats (2 days post-destruction of pancreatic β-cells with 55mg/kg STZ tail vein injection, a time-point when blood glucose levels were >20mM). Glycogen was extracted as previously described.[35] Briefly, tissues were homogenized in glycogen extraction buffer (in mM: 50 Tris pH 8, 150 NaCl, 2 EDTA) and cellular debris was removed by centrifugation (6000 g, 10 minutes, 4 ˚C). The supernatant was ultracentrifuged (300,000 g, 60 minutes, 4 ˚C), and the resulting pellet was resuspended in

glycogen extraction buffer and layered over a sucrose gradient (75, 50, 25 % w/v sucrose) and ultracentrifuged (300,000 g, 2 hours, 4 ˚C). The resulting pellet containing glycogen was resuspended in glycogen extraction buffer. Glycogen-associated proteins were displaced from the glycogen by addition of α1,4 malto-oligosaccharides (maltodextrin, 50 mg/ml) and ultracentrifuged (400,000 g, 20 minutes, 4 ˚C). The supernatant containing proteins eluted from the glycogen were reduced (tris(2-carboxyethyl)phosphine (TCEP), 5 mM), alkylated (iodoacetamide, 10 mM), trypsin-digested (1:75 w/w, Promega) and desalted (HLB µElution plate, Waters) in preparation for liquid chromatography tandem mass spectrometry (LC-MS/MS). LC-MS/MS was performed in micro-flow mode (Eksigent 415 LC, 5600+ TripleTOF Sciex) using a trap column (ChromXP C18CL 10x0.3 mm 5 µm 120 Å; flow rate 10 µL/min, 3 minutes), and an analytical column (ChromXP C18CL 150x0.3 mm 3 µm 120 Å; flow rate 5 µL/min, 30 ˚C). Peptides were eluted in a linear gradient spanning 3-35 % acetonitrile in water (0.1 % Formic Acid) over 60 minutes. MS/MS scans were acquired as previously described.[36] All raw data from the 5600+ TripleTOF mass spectrometer were converted to mzXML using a Sciex Data converter. Data were analyzed using the Sorcerer 2TM-SEQUEST® algorithm (Sage-N Research, Milpitas CA, USA) searched against the concatenated target/decoy Rat Uniprot 2018 reviewed FASTA database[37,38] limited to trypsin-digested peptides, 50 PPM parent ion tolerance, 1 Da fragment ion tolerance, carbamidomethyl of cysteine fixed modification and oxidation of methionine variable modification. Quantitation, validation and normalization was performed using Scaffold 4 on proteins defined by a minimum of 2 proteotypic peptides (5 % false discovery rate) with >99.0 % probability (Protein Prophet algorithm[39]). Relative protein quantification was derived from MS/MS data using spectral counting, subjected to normalized spectral abundance factor (NSAF)[40] and a minimum value of 0 assigned to non-detected proteins. A subset of proteins identified to be i) exclusively detected in control samples, ii) exclusively detected in acute metabolic stress

samples and iii) differentially abundant in acute metabolic stress vs control samples (-0.2 ≤ fold change ((MS/control)-1) ≥ 0.2, $p<0.05$) were used for subsequent analyses. Proteins relating to the contractile apparatus and protein translation GO categories were excluded. Venn diagrams were constructed for cardiac and skeletal muscle datasets to show the number of unique or differentially abundant proteins in control vs acute metabolic stress samples identified from the Scaffold 4 output. Proteins uniquely detected in the acute metabolic stress samples (not detected in control samples) were categorized using Enrichr software[39,41] into GO categories Carbohydrate Metabolic Processes (GO0005975), Fatty Acid Metabolic Processes (GO0006629) and Amino Acid Metabolic Processes (GO0006520) and Log_2 protein abundance presented in a Bubble Chart format. GO analysis (Enrichr) of all uniquely detected and differentially abundant proteins identified the top 7 GO Biological Processes categories associated with the glycogen proteome response to acute STZ for cardiac and skeletal muscle tissues. The normalized spectral counts of the uniquely detected and differentially abundant proteins in the GO category Carbohydrate Metabolic Processes were converted to heatmap intensity for graphical representation.

The MS/MS proteomics data have been deposited to the ProteomeXchange Consortium (http://www.proteomexchange.org)[42] via the PRIDE partner repository with the dataset identifier #PXD009658.

STRING functional network analysis

The glycogen-tagging protein, STBD1, identified to be of importance in the glycogen proteome response to acute metabolic stress, was subjected to STRING protein-protein association network analysis V11.0[43] to identify common pathways or associations for subsequent investigation. Each association identified was based on text-mining and/or experimentally determined evidence in the rat database. The minimum accepted confidence score (minimum probability) for an association was set at 0.7. Primary (max.

10) and secondary (max. 20) interactions were identified and presented as a network graph.

Statistical analysis and reproducibility

Data are presented as mean ± SEM and statistical analysis was performed using Graphpad Prism V9. A description of biological replicates is provided within the figure legends, measurements were taken from discrete samples. Statistical assumptions concerning the data, including normal distribution and similar variation between experimental groups, were examined for appropriateness before statistical tests were performed. All treatments were randomly allocated and investigators were blinded to treatment groups whenever feasible. For comparison between two groups, a 2-sided Student's t-test was used. For assessment between two independent variables, two-way ANOVA with Bonferroni multiple comparisons post-hoc test was used. For correlation analyses Pearson's correlation coefficient was used. A p-value of <0.05 was considered statistically significant.

Data availability

The datasets generated during and/or analyzed during the current study are available from the corresponding author on reasonable request. Correspondence and requests for materials should be addressed to L.M.D.D (lmd@unimelb.edu.au).

References

1. Hoek, A. G. *et al.* Epidemiology of heart failure in diabetes: a disease in disguise. *Diabetologia* **67**, 574–601 (2024).
2. Mellor, K. M. *et al.* Myocardial glycophagy flux dysregulation and glycogen accumulation characterize diabetic cardiomyopathy. *Journal of Molecular and Cellular Cardiology* **189**, 83–89 (2024).
3. Delbridge, L. M. D., Mellor, K. M., Taylor, D. J. & Gottlieb, R. A. Myocardial stress and autophagy: mechanisms and potential therapies. *Nat Rev Cardiol* **14**, 412–425 (2017).
4. Koutsifeli, P. *et al.* Glycogen-autophagy: Molecular machinery and cellular mechanisms of glycophagy. *J Biol Chem* **298**, 102093 (2022).
5. Varma, U., Koutsifeli, P., Benson, V. L., Mellor, K. M. & Delbridge, L. M. D. Molecular mechanisms of cardiac pathology in diabetes - Experimental insights. *Biochim Biophys Acta Mol Basis Dis* **1864**, 1949–1959 (2018).
6. Heather, L. C., Gopal, K., Srnic, N. & Ussher, J. R. Redefining Diabetic Cardiomyopathy: Perturbations in Substrate Metabolism at the Heart of Its Pathology. *Diabetes* **73**, 659–670 (2024).
7. Mellor, K. M., Bell, J. R., Young, M. J., Ritchie, R. H. & Delbridge, L. M. D. Myocardial autophagy activation and suppressed survival signaling is associated with insulin resistance in fructose-fed mice. *J Mol Cell Cardiol* **50**, 1035–1043 (2011).
8. Mellor, K. M., Reichelt, M. E. & Delbridge, L. M. D. Autophagy anomalies in the diabetic myocardium. *Autophagy* **7**, 1263–1267 (2011).
9. Jiang, S., Wells, C. D. & Roach, P. J. Starch-binding domain-containing protein 1 (Stbd1) and glycogen metabolism: Identification of the Atg8 family interacting motif (AIM) in Stbd1 required for interaction with GABARAPL1. *Biochem Biophys Res Commun* **413**, 420–425 (2011).

10. Mellor, K. M., Varma, U., Stapleton, D. I. & Delbridge, L. M. D. Cardiomyocyte glycophagy is regulated by insulin and exposure to high extracellular glucose. *Am. J. Physiol. Heart Circ. Physiol.* **306**, H1240-1245 (2014).
11. Faulkes, C. G. *et al.* Naked mole-rats have distinctive cardiometabolic and genetic adaptations to their underground low-oxygen lifestyles. *Nat Commun* **15**, 2204 (2024).
12. Pierce, G. N. & Philipson, K. D. Binding of glycolytic enzymes to cardiac sarcolemmal and sarcoplasmic reticular membranes. *J Biol Chem* **260**, 6862–6870 (1985).
13. Xu, K. Y., Zweier, J. L. & Becker, L. C. Functional coupling between glycolysis and sarcoplasmic reticulum Ca2+ transport. *Circ Res* **77**, 88–97 (1995).
14. Koutsifeli, P. *et al.* Methods for detection of cardiac glycogen-autophagy. *Autophagy Reports* (2024).
15. Ke, J., Pan, J., Lin, H. & Gu, J. Diabetic cardiomyopathy: a brief summary on lipid toxicity. *ESC Heart Fail* **10**, 776–790 (2023).
16. Jiang, S. *et al.* Starch binding domain-containing protein 1/genethonin 1 is a novel participant in glycogen metabolism. *J Biol Chem* **285**, 34960–34971 (2010).
17. Chandramouli, C. *et al.* Myocardial glycogen dynamics: new perspectives on disease mechanisms. *Clin. Exp. Pharmacol. Physiol.* **42**, 415–425 (2015).
18. Zhang, Y. *et al.* Decoding the molecular mechanism of selective autophagy of glycogen mediated by autophagy receptor STBD1. *Proc Natl Acad Sci U S A* **121**, e2402817121 (2024).
19. Delbridge, L. M. *et al.* Glycophagy — the physiological perspective on a newly characterized glycogen-selective autophagy. *Current Opinion in Physiology* **30**, 100598 (2022).
20. Daniels, L. J. *et al.* Myocardial Energy Stress, Autophagy Induction, and Cardiomyocyte Functional Responses. *Antioxid. Redox Signal.* **31**, 472–486 (2019).

21. Heather, L. C. *et al.* Guidelines on models of diabetic heart disease. *Am J Physiol Heart Circ Physiol* **323**, H176–H200 (2022).
22. Zoppini, G. *et al.* The E/e' ratio difference between subjects with type 2 diabetes and controls. A meta-analysis of clinical studies. *PLoS One* **13**, e0209794 (2018).
23. Kabeya, Y. *et al.* LC3, a mammalian homologue of yeast Apg8p, is localized in autophagosome membranes after processing. *EMBO J* **19**, 5720–5728 (2000).
24. Klionsky, D. J. *et al.* Guidelines for the use and interpretation of assays for monitoring autophagy (4th edition). *Autophagy* **17**, 1–382 (2021).
25. Janssens JV, Raaijmakers AJA, Koutsifeli P, Weeks KL, Bell JR, Van Eyk JE, Curl CL, Mellor KM, Delbridge LMD. Mechanical loading reveals an intrinsic cardiomyocyte stiffness contribution to diastolic dysfunction in murine cardiometabolic disease. *Journal of Physiology* In Press (2024).
26. Mills, R. J. *et al.* Functional screening in human cardiac organoids reveals a metabolic mechanism for cardiomyocyte cell cycle arrest. *Proc Natl Acad Sci U S A* **114**, E8372–E8381 (2017).
27. Voges, H. K. *et al.* Development of a human cardiac organoid injury model reveals innate regenerative potential. *Development* **144**, 1118–1127 (2017).
28. Meddeb, M. *et al.* Myocardial ultrastructure of human heart failure with preserved ejection fraction. *Nat Cardiovasc Res* **3**, 907–914 (2024).
29. Reichelt, M. E., Mellor, K. M., Curl, C. L., Stapleton, D. & Delbridge, L. M. D. Myocardial glycophagy - a specific glycogen handling response to metabolic stress is accentuated in the female heart. *J. Mol. Cell. Cardiol.* **65**, 67–75 (2013).
30. Takeshige, K., Baba, M., Tsuboi, S., Noda, T. & Ohsumi, Y. Autophagy in yeast demonstrated with proteinase-deficient mutants and conditions for its induction. *J Cell Biol* **119**, 301–311 (1992).

31. Abeliovich, H. *et al.* Where is the field of autophagy research heading? *Autophagy* **19**, 1049–1054 (2023).
32. Daniels, L. J. *et al.* Myocardial deformation imaging by 2D speckle tracking echocardiography for assessment of diastolic dysfunction in murine cardiopathology. *Sci Rep* **13**, 12344 (2023).
33. Chandramouli, C. *et al.* Diastolic dysfunction is more apparent in STZ-induced diabetic female mice, despite less pronounced hyperglycemia. *Sci Rep* **8**, 2346 (2018).
34. Mellor, K. M., Wendt, I. R., Ritchie, R. H. & Delbridge, L. M. D. Fructose diet treatment in mice induces fundamental disturbance of cardiomyocyte Ca2+ handling and myofilament responsiveness. *Am. J. Physiol. Heart Circ. Physiol.* **302**, H964-972 (2012).
35. Stapleton, D. *et al.* Analysis of hepatic glycogen-associated proteins. *Proteomics* **10**, 2320–2329 (2010).
36. Parker, S. J., Venkatraman, V. & Van Eyk, J. E. Effect of peptide assay library size and composition in targeted data-independent acquisition-MS analyses. *Proteomics* **16**, 2221–2237 (2016).
37. Apweiler, R. *et al.* UniProt: the Universal Protein knowledgebase. *Nucleic Acids Res* **32**, D115-119 (2004).
38. Elias, J. E. & Gygi, S. P. Target-decoy search strategy for increased confidence in large-scale protein identifications by mass spectrometry. *Nat Methods* **4**, 207–214 (2007).
39. Kuleshov, M. V. *et al.* Enrichr: a comprehensive gene set enrichment analysis web server 2016 update. *Nucleic Acids Res* **44**, W90-97 (2016).
40. Zybailov, B. *et al.* Statistical analysis of membrane proteome expression changes in Saccharomyces cerevisiae. *J Proteome Res* **5**, 2339–2347 (2006).

41. Chen, E. Y. *et al.* Enrichr: interactive and collaborative HTML5 gene list enrichment analysis tool. *BMC Bioinformatics* **14**, 128 (2013).

42. Vizcaíno, J. A. *et al.* The PRoteomics IDEntifications (PRIDE) database and associated tools: status in 2013. *Nucleic Acids Res* **41**, D1063-1069 (2013).

43. Szklarczyk, D. *et al.* STRING v11: protein-protein association networks with increased coverage, supporting functional discovery in genome-wide experimental datasets. *Nucleic Acids Res* **47**, D607–D613 (2019).

Acknowledgements

General: We acknowledge D.Stapleton for providing the glycogen phosphorylase antibodies. **Funding:** This work was supported by grants from the National Health and Medical Research Council of Australia (NHMRCA;1027865, 628643, 1082215, 1037320, 1067869, 1157320), the Diabetes Australia Research Trust, Stem Cells Australia, the National Heart Foundation of Australia (NHFA), the New Zealand Marsden Fund (14-UOA-160, 19-UOA-268), the Health Research Council of New Zealand (19/190) and the University of Auckland Faculty Research Development Fund. Fellowship support is acknowledged from NHMRCA (JEH, RGP, ERP), and Heart Foundation of Australia (ERP, JEH).

Author contributions

L.M.D.D and K.M.M conceived and designed the experiments. K.M.M, U.V., P.K., C.L.C., J.V.J., L.J.D, G.B.B., A.J.A.R., M.A., X.L., S.L.J., D.J.T., K.R., R.J.M., and R.G.P. performed the experiments. K.M.M, U.V., P.K., C.L.C., J.V.J., L.J.D, G.B.B., A.J.A.R., M.A., X.L., S.J., D.J.T., K.R., K.L.W., R.J.M., J.R.B., E.R.P., and J.E.H. analyzed the data. L.M.D.D, K.M.M., E.R.P., J.E.H., J.E.V., X.H, R-P.X and R.A.G. contributed materials/analysis tools. L.M.D.D. and K.M.M wrote the paper.

Competing interests

The authors declare no competing financial interests.

Supplementary information

Extended Data Figure 1. Cardiac function, glycogen synthase and glycogen phosphorylase activity in T2D hearts.
Extended Data Figure 2. AAV9-cTnT-Gabarapl1 in vivo cardiac overexpression in type 2 diabetic (T2D) mice.
Extended Data Table 1. Proteomic (LC-MS/MS) analysis of glycogen-associated proteins in cardiac and skeletal muscle in control and metabolic stress rats.
Extended Data Table 2. Characteristics of the T2D mouse model.
Extended Data Table 3. Primer sequences for glycophagy markers.
Extended Data Table 4. AAV9-cTnT-Gabarapl1 T2D mice: systemic and cardiac characteristics.

Figure legends

Fig.1 | Glycophagy mediator proteins are mobilized early in cardiac glycogen response to metabolic challenge *in vivo*. a, Heart glycogen is increased in rats subjected to an acute metabolic challenge (MC, 48 hr post-streptozotocin injection) and skeletal muscle glycogen is unchanged (n=6-7 rats/group). **b,** Glycogen proteome in cardiac and skeletal (quadriceps) muscle response to an acute metabolic challenge *in vivo*. Venn diagram values show the number of unique or differentially abundant proteins in control (Ctrl) vs metabolic challenge (MC) samples using LC-MS/MS. Total number of significantly up- or down-regulated proteins shown in brackets. n=4 rats/group. **c,** The glycogen proteome response to an acute metabolic challenge is characterized by changes in proteins related to carbohydrate and amino acid metabolism in cardiac muscle, contrasting with skeletal muscle where changes in fatty acid metabolism related proteins are most evident. Data are derived from spectral counts of uniquely present proteins in acute metabolic challenge rat tissue from Carbohydrate (GO:0005975), Fatty Acid (GO:0006629) or Amino Acid (GO:0006520) Metabolic Process GO categories, detected by LC-MS/MS (n=4 rats/group). Bubble size is indicative of protein abundance. **d,** The glycophagy tagging protein, Stbd1 (starch-binding domain-containing protein 1) is detected as a component of the cardiac glycogen proteome only in acute metabolic challenge cardiac muscle (but not in control), whereas Stbd1 is present in both metabolic challenge and control skeletal muscle glycogen proteome. The heatmap is derived from LC-MS/MS normalized spectral counts of differentially abundant or uniquely detected proteins in the Carbohydrate Metabolic Processes GO category (GO:0005975), with normalized spectral abundance factor adjustment (n=4 rats/group). **e,** Glycophagy is identified as a key biological process in the cardiac glycogen proteome response to an acute metabolic challenge *in vivo*. The gene ontology (GO) categories with the highest combined score (Ln(p) x z-score) are presented, comprising glycogen proteome proteins uniquely detected or differentially abundant between metabolic challenge and control for heart and skeletal muscle (n=4 rats/group). **f,** Functional analysis network (STRING) of known and predicted protein interactions with Stbd1. Gabarapl1 is identified as a primary interactor with Stbd1 and a link between glycogen handling and autophagy. Primary interactions are depicted by black outline. Associations are derived from experimental evidence (continuous green line) and text mining evidence (dashed blue line). **g,** Schematic illustrating three stages of glycophagy. Stbd1 tags glycogen and binds to the Atg8 protein, Gabarapl1 (GABA receptor-associated protein-like 1), at the forming glycophagosome membrane. The mature glycophagosome fuses with a lysosome where Gaa (acid α-glucosidase) degrades glycogen to free glucose for metabolic recycling Data are presented as mean ± s.e.m. *$p<0.05$. See also Extended Data Figure 1 and Extended Data Table 1.

Fig.2 | Cardiac GabarapL1 (Atg8) deficiency is associated with diastolic dysfunction in diabetes. a, Diastolic dysfunction (increased echocardiographic index, E/e' ratio) and myocardial glycogen accumulation are evident in type 2 diabetic mice (T2D, high fat diet, n≥10 animals/group). Myocardial glycogen content and diastolic dysfunction (E/e' ratio) are correlated for control (purple) and diabetic (blue, T2D) mice (r, Pearson correlation coefficient). **b,** Cardiac mRNA expression of glycophagy markers in T2D mice. Gabarapl1 is decreased and Stbd1 and Gaa mRNA are unchanged (n=9 animals/group). **c,** Schematic of AAV9 cardiac Gabarapl1 gene delivery in NRVMs. **d,** Confirmation of Gabarapl1 mRNA overexpression with AAV-Gabarapl1 in NRVMs (n=3 independent culture wells/group).
e, Cardiomyocyte glycogen is increased with exposure to high glucose in Null-treated but

not AAV-Gabarapl1 treated cells (n ≥8 independent culture wells/group). Data are presented as mean ± SEM. *p<0.05. See also Extended Data Figure 2 and Extended Data Table 2&3.

Fig.3 | AAV Atg8 gene delivery rescues cardiomyocyte and cardiac diastolic dysfunction in diabetic mice. a, *In vivo* cardiac-specific AAV9-cTnT-Gabarapl1 gene delivery does not affect the development of obesity in T2D mice (high fat diet, n=10 mice/group). **b,** T2D-induced glucose intolerance is not affected by *in vivo* cardiac-specific AAV-Gab gene delivery (high fat diet, n=5-6 mice/group). Baseline (time 0) fasted blood glucose levels are significantly elevated with T2D (2-way ANOVA factor effect). **c,** Cardiac glycogen accumulation in T2D mice is rescued by cardiac Gabarapl1 gene delivery (13 weeks post-AAV injection, high fat diet, presented as fold change vs Ctrl-fed mice for each virus group, n=10-12 mice/group). **d,** T2D-induced diastolic dysfunction (E/e' ratio, echocardiography) is rescued by cardiac Gabarapl1 gene delivery in AAV-transduced mice (high fat diet, presented as fold change vs Ctrl mice for each virus group, n=9-13 mice/group). **e,** Single intact cardiomyocyte force traces (exemplar) show rescued diastolic force (an indicator of passive stiffness) with cardiac Gabarapl1 gene delivery in diabetic mice (AAV9-cTnT-Gabarapl1; T2D, high fat diet; 24 weeks post-AAV injection). **f,** T2D-induced cardiomyocyte diastolic stiffness is rescued by cardiac Gabarapl1 gene delivery in diabetic mice (end-diastolic force-length relation slope; isolated stretched cardiomyocytes from mice at 24 weeks post-AAV injection, high fat diet, n=11-16 cells/group). Data are presented as mean ± s.e.m, *p<0.05. See also Extended Data Figure 3a-c & Extended Data Table 4.

Fig.4 | AAV Atg8 gene delivery improves diastolic performance in 'diabetic' human iPSC-derived cardiac organoids. a, Representative confocal image of a human pluripotent stem cell-derived cardiac organoid, stained for α-actinin (red) and DNA (blue, Hoescht stain). **b,** Transmission electron microscopy images of cardiac organoids showing increased glycogen deposits (black dots) in HG-treated organoids. High magnification image of a glycophagosome in an HG-treated organoid. Scale bar, 1μm. **c,** Exemplar force traces from human cardiac organoids, normalized systolic force. **d,** HG-induced diastolic dysfunction (delayed time to 50% relaxation of force) is rescued by AAV9-Gabarapl1 transduction in human cardiac organoids (n=13-19 organoids/group). **e,** Systolic function (active force production) is unchanged with HG and Gabarapl1 gene delivery (n=13-19 organoids/group). Data are presented as mean ± s.e.m, *p<0.05. See also Extended Data Figure 3d.

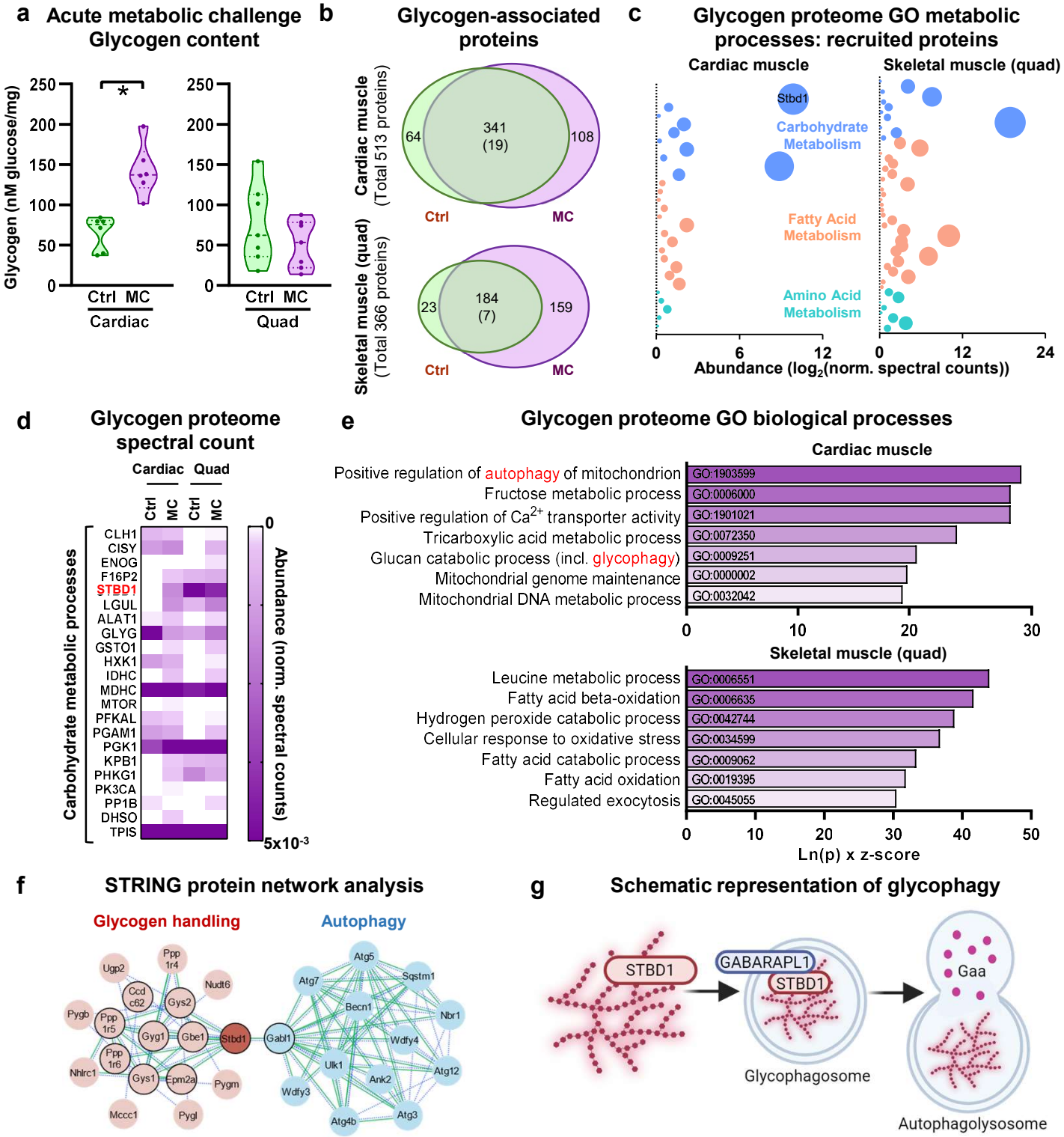

Fig.1 | Glycophagy mediator proteins are mobilized early in cardiac glycogen response to metabolic challenge *in vivo*. a, Heart glycogen is increased in rats subjected to an acute metabolic challenge (MC, 48 hr post-streptozotocin injection) and skeletal muscle glycogen is unchanged (n=6-7 rats/group). **b,** Glycogen proteome in cardiac and skeletal (quadriceps) muscle response to an acute metabolic challenge *in vivo*. Venn diagram values show the number of unique or differentially abundant proteins in control (Ctrl) vs metabolic challenge (MC) samples using LC-MS/MS. Total number of significantly up- or down-regulated proteins shown in brackets. n=4 rats/group. **c,** The glycogen proteome response to an acute metabolic challenge is characterized by changes in proteins related to carbohydrate and amino acid metabolism in cardiac muscle, contrasting with skeletal muscle where changes in fatty acid metabolism related proteins are most evident. Data are derived from spectral counts of uniquely present proteins in acute metabolic challenge rat tissue from Carbohydrate (GO:0005975), Fatty Acid (GO:0006629) or Amino Acid (GO:0006520) Metabolic Process GO categories, detected by LC-MS/MS (n=4 rats/group). Bubble size is indicative of protein abundance. **d,** The glycophagy tagging protein, Stbd1 (starch-binding domain-containing protein 1) is detected as a component of the cardiac glycogen proteome only in acute metabolic challenge cardiac muscle (but not in control), whereas Stbd1 is present in both metabolic challenge and control skeletal muscle glycogen proteome. The heatmap is derived from LC-MS/MS normalized spectral counts of differentially abundant or uniquely detected proteins in the Carbohydrate Metabolic Processes GO category (GO:0005975), with normalized spectral abundance factor adjustment (n=4 rats/group). **e,** Glycophagy is identified as a key biological process in the cardiac glycogen proteome response to an acute metabolic challenge *in vivo*. The gene ontology (GO) categories with the highest combined score (Ln(p) x z-score) are presented, comprising glycogen proteome proteins uniquely detected or differentially abundant between metabolic challenge and control for heart and skeletal muscle (n=4 rats/group). **f,** Functional analysis network (STRING) of known and predicted protein interactions with Stbd1. Gabarapl1 is identified as a primary interactor with Stbd1 and a link between glycogen handling and autophagy. Primary interactions are depicted by black outline. Associations are derived from experimental evidence (continuous green line) and text mining evidence (dashed blue line). **g,** Schematic illustrating three stages of glycophagy. Stbd1 tags glycogen and binds to the Atg8 protein, Gabarapl1 (GABA receptor-associated protein-like 1), at the forming glycophagosome membrane. The mature glycophagosome fuses with a lysosome where Gaa (acid α-glucosidase) degrades glycogen to free glucose for metabolic recycling Data are presented as mean ± s.e.m. *p<0.05. See also Extended Data Figure 1 and Extended Data Table 1.

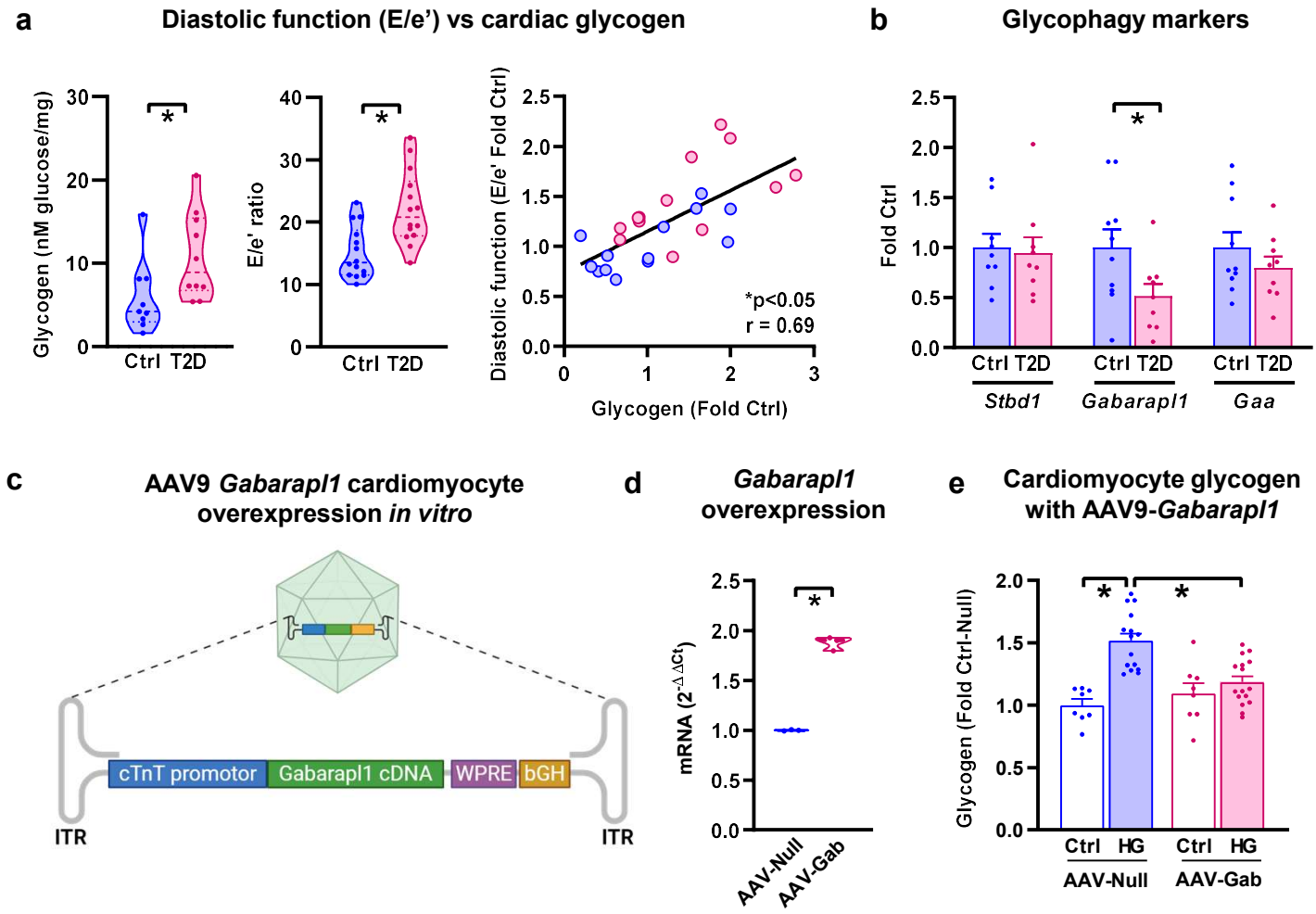

Fig.2 | Cardiac GabarapL1 (Atg8) deficiency is associated with diastolic dysfunction in diabetes. a, Diastolic dysfunction (increased echocardiographic index, E/e' ratio) and myocardial glycogen accumulation are evident in type 2 diabetic mice (T2D, high fat diet, n≥10 animals/group). Myocardial glycogen content and diastolic dysfunction (E/e' ratio) are correlated for control (purple) and diabetic (blue, T2D) mice (r, Pearson correlation coefficient). **b,** Cardiac mRNA expression of glycophagy markers in T2D mice. Gabarapl1 is decreased and Stbd1 and Gaa mRNA are unchanged (n=9 animals/group). **c,** Schematic of AAV9 cardiac Gabarapl1 gene delivery in NRVMs. **d,** Confirmation of Gabarapl1 mRNA overexpression with AAV-Gabarapl1 in NRVMs (n=3 independent culture wells/group). **e,** Cardiomyocyte glycogen is increased with exposure to high glucose in Null-treated but not AAV-Gabarapl1 treated cells (n ≥8 independent culture wells/group). Data are presented as mean ± SEM. *p<0.05. See also Extended Data Figure 2 and Extended Data Table 2&3.

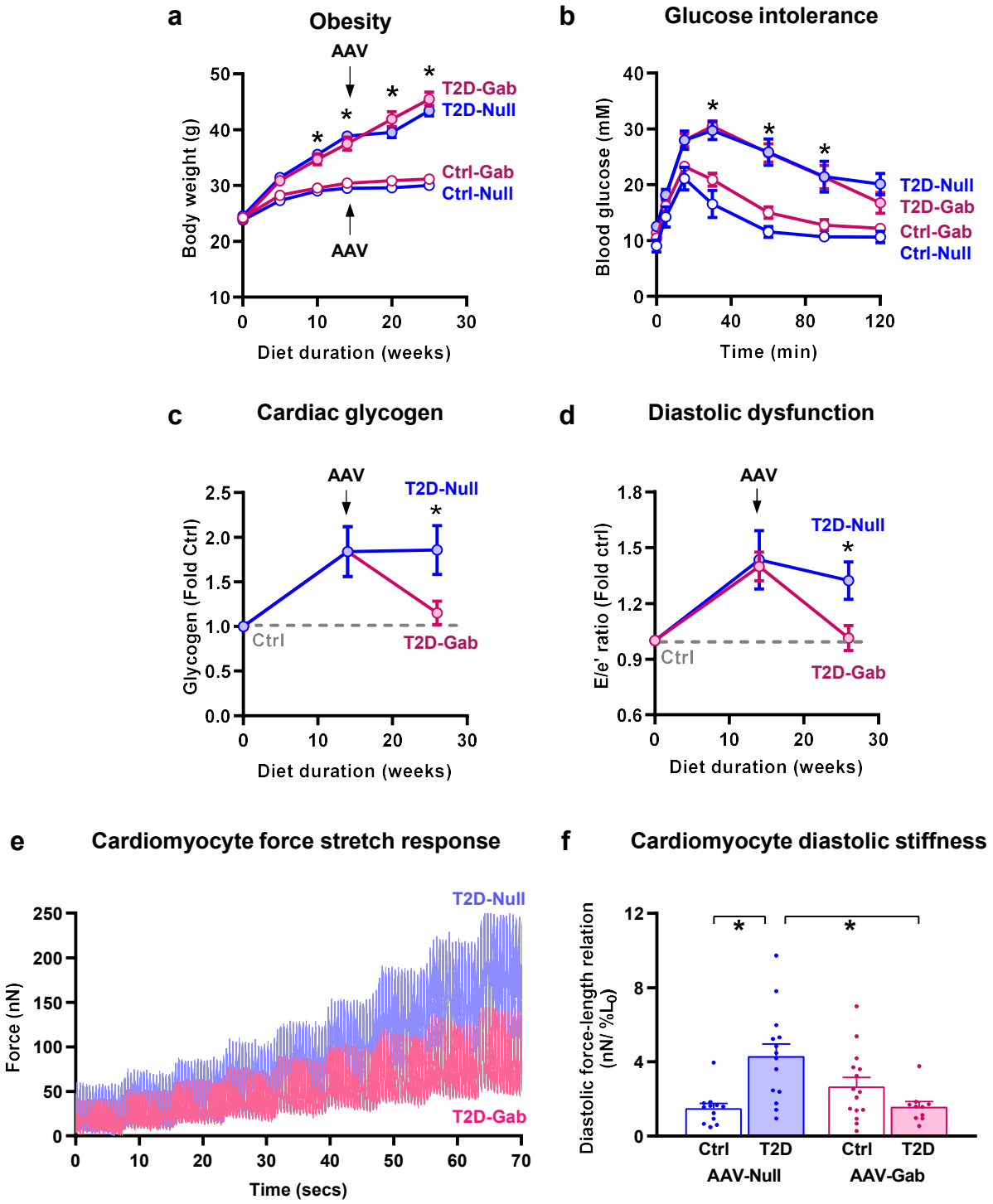

Fig.3 | AAV Atg8 gene delivery rescues cardiomyocyte and cardiac diastolic dysfunction in diabetic mice. a, In vivo cardiac-specific AAV9-cTnT-Gabarapl1 gene delivery does not affect the development of obesity in T2D mice (high fat diet, n=10 mice/group). **b,** T2D-induced glucose intolerance is not affected by in vivo cardiac-specific AAV-Gab gene delivery (high fat diet, n=5-6 mice/group). Baseline (time 0) fasted blood glucose levels are significantly elevated with T2D (2-way ANOVA factor effect). **c,** Cardiac glycogen accumulation in T2D mice is rescued by cardiac Gabarapl1 gene delivery (13 weeks post-AAV injection, high fat diet, presented as fold change vs Ctrl-fed mice for each virus group, n=10-12 mice/group). **d,** T2D-induced diastolic dysfunction (E/e' ratio, echocardiography) is rescued by cardiac Gabarapl1 gene delivery in AAV-transduced mice (high fat diet, presented as fold change vs Ctrl mice for each virus group, n=9-13 mice/group). **e,** Single intact cardiomyocyte force traces (exemplar) show rescued diastolic force (an indicator of passive stiffness) with cardiac Gabarapl1 gene delivery in diabetic mice (AAV9-cTnT-Gabarapl1; T2D, high fat diet; 24 weeks post-AAV injection). **f,** T2D-induced cardiomyocyte diastolic stiffness is rescued by cardiac Gabarapl1 gene delivery in diabetic mice (end-diastolic force-length relation slope; isolated stretched cardiomyocytes from mice at 24 weeks post-AAV injection, high fat diet, n=11-16 cells/group). Data are presented as mean ± s.e.m, *p<0.05. See also Extended Data Figure 3a-c & Extended Data Table 4.

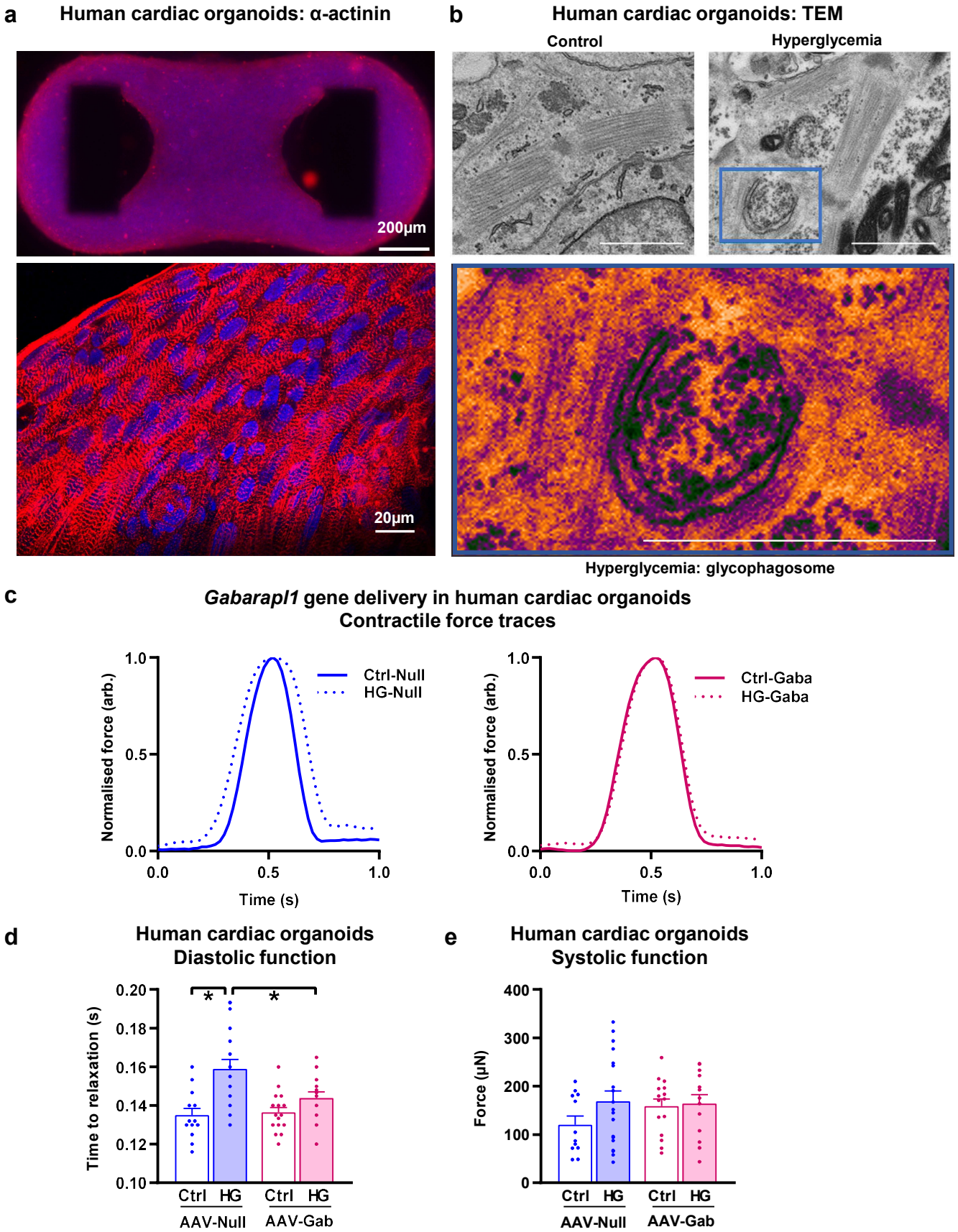

Fig.4 | AAV Atg8 gene delivery improves diastolic performance in 'diabetic' human iPSC-derived cardiac organoids. a, Representative confocal image of a human pluripotent stem cell-derived cardiac organoid, stained for α-actinin (red) and DNA (blue, Hoescht stain). **b,** Transmission electron microscopy images of cardiac organoids showing increased glycogen deposits (black dots) in HG-treated organoids. High magnification image of a glycophagosome in an HG-treated organoid. Scale bar, 1μm. **c,** Exemplar force traces from human cardiac organoids, normalized systolic force. **d,** HG-induced diastolic dysfunction (delayed time to 50% relaxation of force) is rescued by AAV9-Gabarapl1 transduction in human cardiac organoids (n=13-19 organoids/group). **e,** Systolic function (active force production) is unchanged with HG and Gabarapl1 gene delivery (n=13-19 organoids/group). Data are presented as mean ± s.e.m, *p<0.05. See also Extended Data Figure 3d.